

See discussions, stats, and author profiles for this publication at: <https://www.researchgate.net/publication/38079656>

Graphene Oxide Amplified Electrogenenerated Chemiluminescence of Quantum Dots and Its Selective Sensing for Glutathione from Thiol-Containing Compounds

ARTICLE *in* ANALYTICAL CHEMISTRY · NOVEMBER 2009

Impact Factor: 5.64 · DOI: 10.1021/ac901935a · Source: PubMed

CITATIONS

233

READS

200

5 AUTHORS, INCLUDING:



Jin Lu

Arizona State University

15 PUBLICATIONS 1,767 CITATIONS

SEE PROFILE



Haixin Chang

Huazhong University of Science and Techn...

26 PUBLICATIONS 1,654 CITATIONS

SEE PROFILE

Graphene Oxide Amplified Electrogenenerated Chemiluminescence of Quantum Dots and Its Selective Sensing for Glutathione from Thiol-Containing Compounds

Ying Wang, Jin Lu, Longhua Tang, Haixin Chang, and Jinghong Li*

Department of Chemistry, Key Laboratory of Bioorganic Phosphorus Chemistry and Chemical Biology, Tsinghua University, Beijing 100084, China

Here we report a graphene oxide amplified electrogenerated chemiluminescence (ECL) of quantum dots (QDs) platform and its efficient selective sensing for antioxidants. Graphene oxide facilitated the CdTe QDs^{•+} production and triggered O₂^{•-} generation. Then, a high yield of CdTe QDs* was formed due to the combination of CdTe QDs^{•+} and O₂^{•-}, leading to an ~5-fold ECL amplification. Glutathione is the most abundant cellular thiol-containing peptide, but its selective sensing is an intractable issue in analytical and biochemical communities because its detection is interfered with by some thiol-containing compounds. This platform showed a detection limit of 8.3 μM (S/N = 3) for glutathione and a selective detection linear dependence from 24 to 214 μM in the presence of 120 μM cysteine and glutathione disulfide. This platform was also successfully used for real sample (eye drug containing glutathione) detection without any pretreatment with a wide linear range from 0.04 to 0.29 μg mL⁻¹.

Electrogenenerated chemiluminescence (ECL) is a light emission that arises from the high-energy electron-transfer reaction between electrogenerated species.¹ According to the different luminophor categories, ECL systems could be divided into inorganic systems (e.g., Ru(bpy)₃²⁺), organic systems (e.g., luminol), and quantum dot (QD) systems.^{2,3} Due to the unique quantum size dependent electrochemical properties of QDs^{4,5} and controllable ECL merits,² QDs ECL has become more and more fascinating. Such ECL of various QDs like CdTe,⁶ CdSe,⁷ and PbS⁸ has been extensively

investigated in biochemical and analytical communities⁹ and profoundly used for catechol derivatives detection,¹⁰ DNA detection,¹¹ and immunoassay.¹² However, the narrow potential window due to the aqueous solvent for biosensings² and the instability of the generated QDs radical species restricted the further application of QDs ECL systems in analysis. In the previous works, some oxidants including K₂S₂O₈,¹² H₂O₂,¹³ and Na₂SO₃¹⁴ were usually selected to improve the ECL systems. Although the ECL intensity was enhanced, these oxidants would destroy the buffer condition and even oxidize all of the analytes, making the systems lose selectivity and biocompatibility.¹³ Hence, a new pathway is highly desirable to meliorate the QDs ECL systems.

Graphene oxide^{15,16} is a chemically modified graphene sheet containing oxygen functional groups such as epoxide, alcohol, and carboxylic acid. In our previous studies, we found the unique planar structure of graphene displayed nice properties in electrochemistry^{17,18} and realized the selective probing of dopamine.¹⁹ Graphene oxide not only owns the two-dimensional structure like graphene but also possesses some properties totally different from graphene such as hydrophilicity,²⁰ multiple oxygen moieties,²¹ and controllable electronic properties.²² In view of the graphene oxide researches about molecular sensors,²³ drug

* To whom correspondence should be addressed. E-mail: jhli@mails.tsinghua.edu.cn.

- (1) Richter, M. M. *Chem. Rev.* **2004**, *104*, 3003–3036.
- (2) Miao, W. *Chem. Rev.* **2008**, *108*, 2506–2553.
- (3) Bertonecello, P.; Forster, R. J. *Biosens. Bioelectron.* **2009**, *24*, 3191–3200.
- (4) Michalek, X.; Pinaud, F. F.; Bentolila, L. A.; Tsay, J. M.; Dooze, S.; Li, J. J.; Sundaresan, G.; Wu, A. M.; Gambhir, S. S.; Weiss, S. *Science* **2005**, *307*, 538–544.
- (5) Clapp, A. R.; Goldman, E. R.; Mattoussi, H. *Nat. Protoc.* **2006**, *1*, 1258–1267.
- (6) Bae, Y.; Myung, N.; Bard, A. J. *Nano Lett.* **2004**, *4*, 1153–1161.
- (7) Ding, S. N.; Xu, J. J.; Chen, H. Y. *Chem. Commun.* **2006**, (34), 3631–3633.
- (8) Sun, L.; Bao, L.; Hyun, B.; Bartnik, A. C.; Zhong, Y.; Reed, J. C.; Pang, D.; Abruna, H. D.; Malliaras, G. G.; Wise, F. W. *Nano Lett.* **2009**, *9*, 789–793.

- (9) Hazelton, S. G.; Zheng, X.; Zhao, J. X.; Pierce, D. T. *Sensors* **2008**, *8*, 5942–5960.
- (10) Jiang, H.; Ju, H. *Anal. Chem.* **2007**, *79*, 8055–8060.
- (11) Shan, Y.; Xu, J.; Chen, H. Y. *Chem. Commun.* **2009**, (8), 905–907.
- (12) Jie, G. F.; Huang, H. P.; Sun, X. L.; Zhu, J. J. *Biosens. Bioelectron.* **2008**, *23*, 1896–1899.
- (13) Jiang, H.; Ju, H. *Anal. Chem.* **2007**, *79*, 6690–6696.
- (14) Liu, X.; Ju, H. *Anal. Chem.* **2008**, *80*, 5377–5382.
- (15) Cote, L. J.; Kim, F.; Huang, J. J. *Am. Chem. Soc.* **2009**, *131*, 1043–1049.
- (16) Dikin, D. A.; Stankovich, S.; Zimney, E. J.; Piner, R. D.; Dommett, G. H. B.; Evmenenko, G.; Nguyen, S. T.; Ruoff, R. S. *Nature* **2007**, *448*, 457–460.
- (17) Xia, J. L.; Chen, F.; Li, J. H.; Tao, N. J. *Nat. Nanotechnol.* **2009**, *4*, 505–509.
- (18) Tang, L. H.; Wang, Y.; Li, Y. M.; Feng, H.; Lu, J.; Li, J. H. *Adv. Funct. Mater.* **2009**, *19*, 2782–2789.
- (19) Wang, Y.; Li, Y.; Tang, L.; Lu, J.; Li, J. H. *Electrochem. Commun.* **2009**, *11*, 889–892.
- (20) Becerril, H. A.; Mao, J.; Liu, Z.; Stoltenberg, R. M.; Bao, Z.; Chen, Y. *ACS Nano* **2008**, *2*, 463–470.
- (21) Mkhoyan, K. A.; Contryman, A. W.; Silcox, J.; Stewart, D. A.; Eda, G.; Mattevi, C.; Miller, S.; Chhowalla, M. *Nano Lett.* **2009**, *9*, 1058–1063.
- (22) Gómez-Navarro, C.; Weitz, R. T.; Bittner, A. M.; Scolari, M.; Mews, A.; Burghard, M.; Kern, K. *Nano Lett.* **2007**, *7*, 3499–3503.
- (23) Robinson, J. T.; Perkins, F. K.; Snow, E. S.; Wei, Z.; Sheehan, P. E. *Nano Lett.* **2008**, *8*, 3137–3140.

delivery assistants,²⁴ and the ECL study with tri-*n*-propylamine,²⁵ its controllable oxidation and the corresponding electronic properties have also been released.

Selective detection of glutathione is expected imminently to biomedical and analytical communities.^{26,27} (i) Glutathione (γ -Glu-Cys-Gly, GSH) is the most abundant cellular thiol-containing compound,^{28,29} and its level is directly related with cellular damage, some diseases, and food degradation; (ii) GSH detection is interfered by cysteine (Cys) and glutathione disulfide (GSSG). Hereinto, Cys is the common source of the sulfur atom of sulfur-containing peptides and GSSG is the oxidative form of GSH in physiological fluids.³⁰ Generally, current methods for GSH detection are capillary electrophoresis, or high-performance liquid chromatography associated with fluorescence or UV detection, and electrochemistry.³¹ To obtain the selectivity, different derivatization reagents or a mass-selective detector must be used for the first two kinds. Unfortunately, derivatization reagents make the system so complicated, and the mass-selective detector is expensive and needs experienced laboratory personnel.³² Electrochemical methods offer an attractive alternative due to the low cost and simplicity but suffer from the similar redox potential of GSH and Cys. Although various modified electrodes such as a DNA-modified electrode,³³ tubular-wire dual electrode,³⁴ and poly Eugenol-modified glassy carbon electrode³⁵ have been developed to solve this problem, the selective detection of GSH is still an issue demanding prompt solution especially with the interferences from Cys and GSSG.

In the present work, we proposed a graphene oxide amplified ECL platform where graphene oxide facilitated the generation of QDs radicals and formed a high yield of QDs*, then leading to an ~ 5 times enhancement of ECL intensity compared with the system without graphene oxide. Furthermore, the proposed platform also exhibited well in glutathione-selective sensing from thiol-containing compounds with a wide linear relationship. This platform was also utilized for glutathione-containing drug detection without any pretreatment. Our experiments displayed the powerful utility of graphene oxide to ECL studies and would emerge eximious applications in analytical and biochemical communities.

EXPERIMENTAL SECTION

Chemicals and Synthesis. Glutathione, glutathione disulfide, L-cysteine, methionine, and superoxide dismutase (from bovine

erythrocytes, 3000 units mg^{-1} , solid) were from Sigma. Tathion eye drops (Isethion, 5 mL/100 mg) was from ISEI Company, Yamagata, Japan. Other chemicals, Na_2CO_3 , NaHCO_3 , KNO_3 , CdCl_2 , NaHB_4 , H_2SO_4 , $\text{K}_2\text{S}_2\text{O}_8$, P_2O_5 , KMnO_4 , H_2O_2 , HCl , and dimethylformamide (DMF) were from Beijing Chemical Company. All stock solutions were prepared using deionized water. Te powder and thioglycolic acid (TGA) were purchased from Acros Organics (Geel, Belgium). CdTe QDs were synthesized according to the procedure described in our previous works.^{36,37} Graphite powder (99.9%, 325 mesh) was purchased from Alfa Aesar, and graphene oxide was prepared according to the Hummers and Offeman method.³⁸

Characterization. Cyclic voltammograms (CVs) were carried with the CHI 440 (CH Instruments, Inc., Austin, TX). The indium–tin oxide (ITO) electrode with 1 cm width and 2 cm length was purchased from Shenzhen Nanbo Group and acted as the working electrode. It was rinsed with acetone, ethanol, and water orderly before used. A Ag/AgCl with saturated KCl solution acted as the reference electrode, and platinum wire acted as the counter electrode, respectively. The electrochemiluminescence (ECL) measurements were obtained on an MPI-B multifunctional electrochemical analytical system (Xi'an Remex Analytical Instrument Ltd. Co., China). Measurements were carried via the bare ITO electrode as the working electrode, prepared by the same methods which were used for the CV experiments. A Ag/AgCl with saturated KCl solution acted as the reference electrode, and platinum wire acted as the counter electrode. The curves were background-subtracted using ORIGIN 7.0 (Micirocal Software, Northampton, MA) through extrapolation to the baseline in the regions far from the peaks.

The method of computational chemistry was used to verify the binding energy. Configurations of GSH, Cys, and GSSG were optimized by molecular mechanics after the molecular dynamics simulation by the OPLS-2005 force field with MacroModel software³⁹ (step size 1.5 fs, simulation time 1 ns). Binding energy was calculated by the PM3 semiempirical method of Gaussian software⁴⁰ for GSH, Cys, and GSSG with their optimization configurations.

RESULTS AND DISCUSSION

Graphene Oxide Amplified CdTe QDs ECL. As shown in Figure 1A, oxidation current of QDs with $1.2 \mu\text{g mL}^{-1}$ graphene oxide (curve c) is 23 mA at 1.08 V, higher than CdTe QDs

- (24) Liu, Z.; Robinson, J. T.; Sun, X.; Dai, H. *J. Am. Chem. Soc.* **2008**, *130*, 10876–10877.
- (25) Fan, F. F.; Park, S.; Zhu, Y.; Ruoff, R. S.; Bard, A. J. *J. Am. Chem. Soc.* **2009**, *131*, 937–939.
- (26) Safavi, A.; Maleki, N.; Farjami, E.; Mahyari, F. A. *Anal. Chem.* **2009**, *81*, 7538–7543.
- (27) Huang, G. G.; Han, X. X.; Hossain, M. K.; Ozaki, Y. *Anal. Chem.* **2009**, *81*, 5881–5888.
- (28) White, P. C.; Lawrence, N. S.; Davis, J.; Compton, R. G. *Electroanalysis* **2002**, *14*, 89–98.
- (29) Kizek, R.; Vacek, J.; Trnková, L.; Jelen, F. *Bioelectrochemistry* **2004**, *63*, 19–24.
- (30) Rahman, I.; Kode1, A.; Biswas, S. K. *Nat. Protoc.* **2006**, *1*, 3159–3165.
- (31) Kruusma, J.; Benham, A. M.; Williams, J. A. G.; Kataký, R. *Analyst* **2006**, *131*, 459–473.
- (32) Seiwert, B.; Karst, U. *Anal. Chem.* **2007**, *79*, 7131–7138.
- (33) Liu, J.; Roussel, C.; Lagger, G.; Tacchini, P.; Girault, H. H. *Anal. Chem.* **2005**, *77*, 7687–7694.
- (34) Zhong, M.; Lunte, S. M. *Anal. Chem.* **1999**, *71*, 251–255.
- (35) Okumura, L. L.; Stradiotto, N. R.; Rees, N. V.; Compton, R. G. *Electroanalysis* **2008**, *20*, 916–918.

- (36) Li, J.; Hong, X.; Li, D.; Zhao, K.; Wang, L.; Wang, H.; Du, Z.; Li, J. H.; Bai, Y.; Li, T. *Chem. Commun.* **2004**, 1740–1741.
- (37) Li, J.; Hong, X.; Liu, Y.; Li, D.; Wang, Y.; Li, J. H.; Bai, Y.; Li, T. *Adv. Mater.* **2005**, *17*, 163–166.
- (38) Hummers, W. S.; Offeman, R. E. *J. Am. Chem. Soc.* **1958**, *80*, 1339.
- (39) MacroModel, version 9.1; Schrödinger, LLC: New York, 2005.
- (40) Frisch, M. J.; Trucks, G. W.; Schlegel, H. B.; Scuseria, G. E.; Robb, M. A.; Cheeseman, J. R.; Montgomery, J. A., Jr.; Vreven, T.; Kudin, K. N.; Burant, J. C.; Millam, J. M.; Iyengar, S. S.; Tomasi, J. J.; Barone, V.; Mennucci, B.; Cossi, M.; Scalmani, G.; Rega, N.; Petersson, G. A.; Nakatsuji, H.; Hada, M.; Ehara, M.; Toyota, K.; Fukuda, R.; Hasegawa, J.; Ishida, M.; Nakajima, T.; Honda, Y.; Kitao, O.; Nakai, H.; Klene, M.; Li, X.; Knox, J. E.; Hratchian, H. P.; Cross, J. B.; Adamo, C.; Jaramillo, J.; Gomperts, R.; Stratmann, R. E.; Yazyev, O.; Austin, A. J.; Cammi, R.; Pomelli, C.; Ochterski, J. W.; Ayala, P. Y.; Morokuma, K.; Voth, A.; Salvador, P.; Dannenberg, J. J.; Zakrzewski, V. G.; Dapprich, S.; Daniels, A. D.; Strain, M. C.; Farkas, O.; Malick, D. K.; Rabuck, A. D.; Raghavachari, K.; Foresman, J. B.; Ortiz, J. V.; Cui, Q.; Baboul, A. G.; Clifford, S.; Cioslowski, J.; Stefanov, B. B.; Liu, G.; Liashenko, A.; Piskorz, P.; Komaromi, I.; Martin, R. L.; Fox, D. J.; Keith, T.; Al-Laham, M. A.; Peng, C. Y.; Nanayakkara, A.; Challacombe, M.; Gill, P. M. W.; Johnson, B.; Chen, W.; Wong, M. W.; Gonzalez, C.; Pople, J. A. *Gaussian 03*, revision D.01; Gaussian, Inc.: Wallingford, CT and Pittsburgh, PA, 2004.

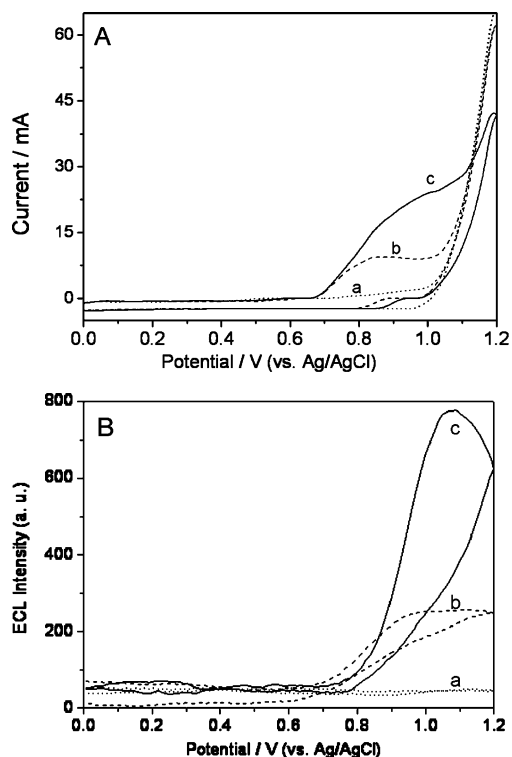


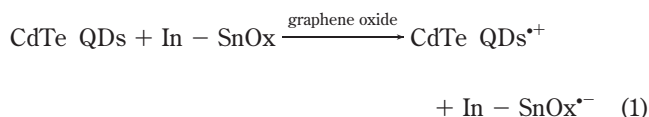
Figure 1. (A) Cyclic voltammograms and (B) ECL intensity–potential behaviors of (a) background, (b) CdTe QDs, and (c) CdTe QDs with $1.2 \mu\text{g mL}^{-1}$ graphene oxide in $0.02 \text{ M Na}_2\text{CO}_3\text{--NaHCO}_3$ (pH 9.5) buffer solution: scan rate, 100 mV s^{-1} .

(curve b, 7 mA). It indicates that graphene oxide facilitates the CdTe QDs oxidation on the ITO electrode. Because ECL is a light emission that arises from the electron-transfer reaction between electrogenerated species, a significant ECL signal of QDs with graphene oxide (curve c) is observed as shown in Figure 1B. On the other hand, no obvious ECL signal is observed from the $1.2 \mu\text{g mL}^{-1}$ graphene oxide in the buffer solution only (shown as Supporting Information Figure S1). In ECL studies, there are two main mechanisms: one is ion annihilation ECL and another is coreactant ECL. As we know, control oxidation and multioxygenic moieties provide tunability of the electronic and mechanical properties of graphene oxide. Thus, we propose that graphene oxide can accelerate the radical species generation, act as the media in emission section, and then amplify the QDs ECL intensity. To confirm the mechanism, we investigate the effects of $\text{O}_2^{\bullet-}$ and O_2 on this system. Superoxide dismutase (SOD), a typical $\text{O}_2^{\bullet-}$ capture, is added into the air-saturated solution to test the effect of $\text{O}_2^{\bullet-}$. As shown in Figure 2, parts A and B, CdTe QDs with graphene oxide (Figure 2A) and CdTe QDs (Figure 2B) show a big ECL intensity decrease, indicating that $\text{O}_2^{\bullet-}$ is necessary for both of them. However, when the ECL experiments are carried out in nitrogen-saturated solution, CdTe QDs with graphene oxide (Figure 2C) show no changes but CdTe QDs (Figure 2D) still show a big decrease in the ECL intensity. It demonstrates that graphene oxide facilitates the $\text{O}_2^{\bullet-}$ production so that trace oxygen dissolved in the solvent is sufficient for ECL generation.

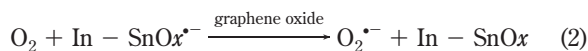
Information about the energy level and band gap is important for reactions and irradiations. The maximum absorption wave-

length of CdTe QDs at 543 nm (Supporting Information Figure S3A) demonstrates its band gap was 2.3 eV .⁴¹ Although graphene-based systems usually have zero band gap, graphene oxide is various in energy gaps because of the tunable oxidation.⁴² Previous studies^{25,43} have pointed out the energy gaps of graphene oxide are diverse from 1.7 to 4.1 eV. So the band gaps of CdTe QDs and graphene oxide are approximative with each other. According to the Mott–Schottky plots (Supporting Information Figure S3B), we find the Fermi level of CdTe QDs is 0.7 eV, which is much more than that of ITO of 3.7 eV (with a band gap of 3.5 eV ⁴⁴), but graphene oxide owns the 0.9 eV Fermi level which is also approximative to QDs. Hence, graphene oxide might be a good intermedium for electron transfer from CdTe QDs to ITO electrode.

Equations corresponding to each step of the emission process are obtained. CdTe QDs oxidation is facilitated by graphene oxide:



Then, $\text{O}_2^{\bullet-}$ production is also facilitated by graphene oxide:



The combination of positive and negative radical species leads to the formation of CdTe QDs*. Considering graphene oxide can promote the productions of CdTe QDs*⁺ and $\text{O}_2^{\bullet-}$, and improve the radical species stability, a high yield of CdTe QDs* is released, and finally amplification of ECL intensity is observed:



Optimum of Graphene Oxide Concentration and pH. The ECL efficiencies were strongly influenced by the assay conditions, such as graphene oxide concentration or pH of the buffer solution. So effects of graphene oxide concentration and pH were investigated in the next works. Supporting Information Figure S4A shows the effect of graphene oxide concentration from 0 to $2.5 \mu\text{g mL}^{-1}$ on the ECL readout of the amplified ECL platform. ECL intensity increased significantly as the graphene oxide concentration up to $1.2 \mu\text{g mL}^{-1}$, reflecting the improved ECL efficiency. However, no signal enhancement could be observed when the graphene oxide concentration was up to more than $1.5 \mu\text{g mL}^{-1}$. Next, the effect of pH was examined as shown in Supporting Information Figure S4B. The ECL signals increased from pH 7 to pH 9.5 and then went down with more alkaline. Therefore, $1.2 \mu\text{g mL}^{-1}$ and pH 9.5 were chosen as the optimum

(41) Gassenbauer, Y.; Wachau, A.; Klein, A. *Phys. Chem. Chem. Phys.* **2009**, *11*, 3049–3054.

(42) Jin, M.; Jeong, H.-K.; Yu, W.; Bae, D.; Kang, B.; Lee, Y. *J. Phys. D: Appl. Phys.* **2009**, *42*, 135109–135114.

(43) Boukhvalov, D. W.; Katsnelson, M. I. *J. Am. Chem. Soc.* **2008**, *130*, 10697–10701.

(44) Coe, S.; Woo, W.; Bawendi, M.; Bulovic, V. *Nature* **2002**, *420*, 800–803.

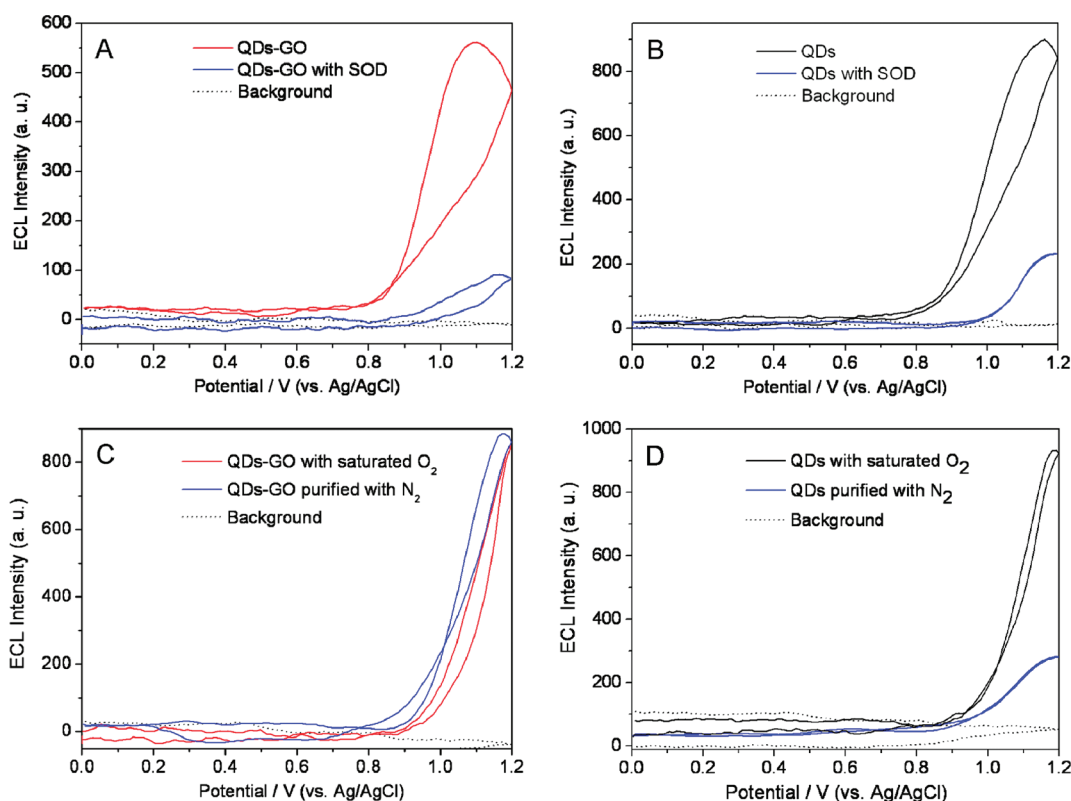


Figure 2. Effect of superoxide radical (A and B) and oxygen (C and D) on the ECL responses of QDs-GO (CdTe QDs with graphene oxide) and CdTe QDs: (A) ECL responses of QDs-GO before (red line) and after the addition of $24 \mu\text{g mL}^{-1}$ SOD (blue line); (B) ECL responses of CdTe QDs before (black line) and after the addition of SOD (blue line); (C) ECL responses of QDs-GO before (red line) and after being nitrogen-saturated (blue line); (D) ECL responses of CdTe QDs before (black line) and after being nitrogen-saturated (blue line) in the $0.02 \text{ M Na}_2\text{CO}_3\text{--NaHCO}_3$ buffer solution (pH 9.5): scan rate, 100 mV s^{-1} . Dot lines in these figures are for the background responses.

Selective Sensing of Glutathione. GSH is the most abundant thiol species in the cytoplasm (the intracellular GSH concentration is from 1 to 10 mM ⁴⁵) and the major reducing agent in biochemical processes, providing a potential in situ releasing source in living cells. Hence sensitive detection of GSH is highly desirable in analytical chemistry. As shown in Figure 3A, graphene oxide amplified ECL showed a rapid intensity decrease while CdTe QDs showed no changes as the glutathione concentration was increasing. The ECL intensity of CdTe QDs with graphene oxide intended to complete quenching as the GSH concentration of $214 \mu\text{M}$ (Figure 3B). According to the Stern–Volmer equation,⁴⁶ $I_0/I = 1 + K_{\text{sv}}[Q]$, where K_{sv} is called the quenching constant, I is the intensity at the quencher concentration $[Q]$, and I_0 is the initial intensity without quencher, the linear dependence of I_0/I on glutathione concentration is obtained as shown in Figure 3C.

Moreover, GSH detection is interfered by Cys and GSSG, because Cys is the sulfur resource of the GSH synthesis and GSSG is the oxidation form of GSH. So selective sensing is also an essential request for GSH detection. To realize the selectivity, various materials such as gold nanoparticles,⁴⁷ rosamine,⁴⁸ methyl

viologen,⁴⁹ and multifarious techniques including fluorescence, chromatography, and electrochemistry have been employed. However, because Cys, GSH, and GSSG owned the similar functional groups (e.g., $-\text{SH}$, $-\text{COOH}$, $-\text{NH}_2$), selective detection of GSH is difficult to carry out via the routine methods. On our trials, the graphene oxide amplified QDs ECL was able to probe GSH in the presence of massive Cys and GSSG. As shown in Figure 4A, a great decrease of ECL intensity of CdTe QDs with graphene oxide was corresponding to $120 \mu\text{M}$ GSH, but no quenching was observed for $120 \mu\text{M}$ Cys or $120 \mu\text{M}$ GSSG. This platform also displayed excellent selectivity and good stability as shown in Figure 4B. The ECL intensity showed little change ($\pm 50 \text{ au}$) for whichever Cys or GSSG but a linear decrease for GSH as the concentrations were increasing. The interfering effect of methionine on the GSH-selective detection was also investigated as shown in Supporting Information Figure S5 because methionine is one of two sulfur-containing proteinogenic amino acids together with cysteine and an intermediate in the biosynthesis of cysteine. No obvious ECL quenching was observed when we added methionine ($120 \mu\text{M}$) into the solution. However, to the same concentration ($120 \mu\text{M}$) of glutathione, a sharp decrease of the ECL intensity was obtained based on the proposed graphene oxide amplified QDs ECL platform.

Next, we investigated the possible reasons leading to the selectivity of this platform. As we know, the structure of graphene

(45) Hong, R.; Han, G.; Fernández, J. M.; Kim, B.; Forbes, N. S.; Rotello, V. M. *J. Am. Chem. Soc.* **2006**, *128*, 1078–1079.

(46) Boaz, H.; Rollefson, G. K. *J. Am. Chem. Soc.* **1950**, *72*, 3435–3443.

(47) Sudeep, P. K.; Shibui, J. S. T.; Thomas, K. G. *J. Am. Chem. Soc.* **2005**, *127*, 6516–6517.

(48) Ahn, Y.; Lee, J.; Chang, Y. *J. Am. Chem. Soc.* **2007**, *129*, 4510–4511.

(49) Wang, W.; Escobedo, J. O.; Lawrence, C. M.; Strongin, R. M. *J. Am. Chem. Soc.* **2004**, *126*, 3400–3401.

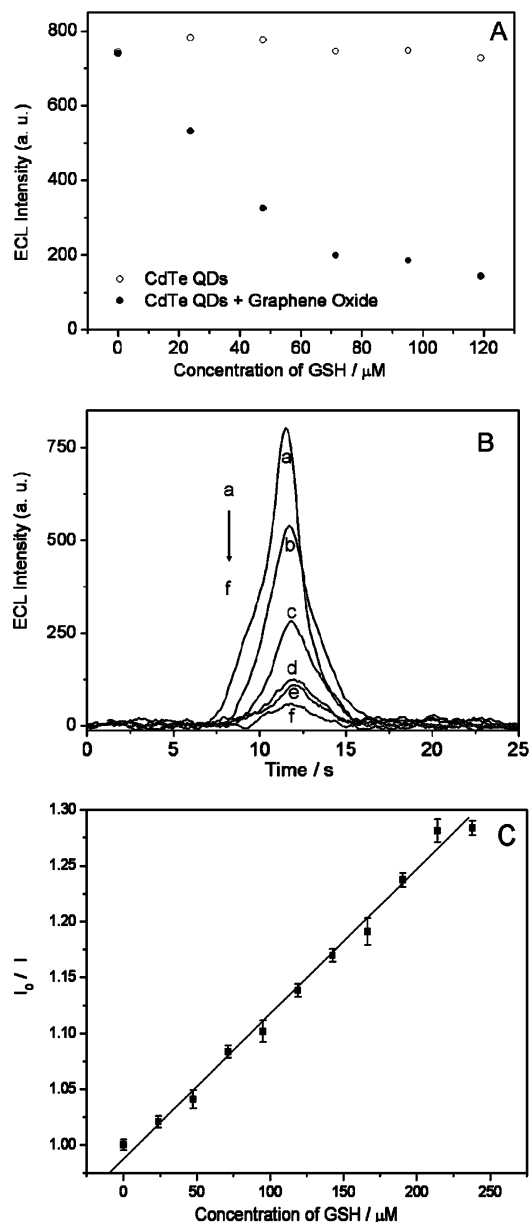


Figure 3. (A) ECL intensities (height of the ECL peak) of CdTe QDs (○) and CdTe QDs with $1.2 \mu\text{g mL}^{-1}$ graphene oxide (●) to different concentrations of glutathione. (B) ECL intensity–time behaviors of (a) CdTe QDs with $1.2 \mu\text{g mL}^{-1}$ graphene oxide for (from b to f) 31, 62, 93, 124, and 155 μM glutathione in 0.02 M Na_2CO_3 – NaHCO_3 (pH 9.5). (C) Linear relationship between the relative ECL intensity (I_0/I) and the concentration of glutathione from 21 to 239 μM . Error bars were calculated from three times parallel experiments.

oxide is assumed to be a graphene sheet bonded to oxygen in the form of carboxyl, hydroxyl, or epoxy groups.⁵⁰ Hydrogen bonds will be formed between these moieties and GSH (Supporting Information Scheme S1, displayed by dashed lines). So binding energies were calculated by computational chemistry based on the optimized configurations of GSH, Cys, and GSSG (by molecular mechanics after the molecular dynamics simulation with Macromodel software: step size 1.5 fs, simulation time 1 ns). Table

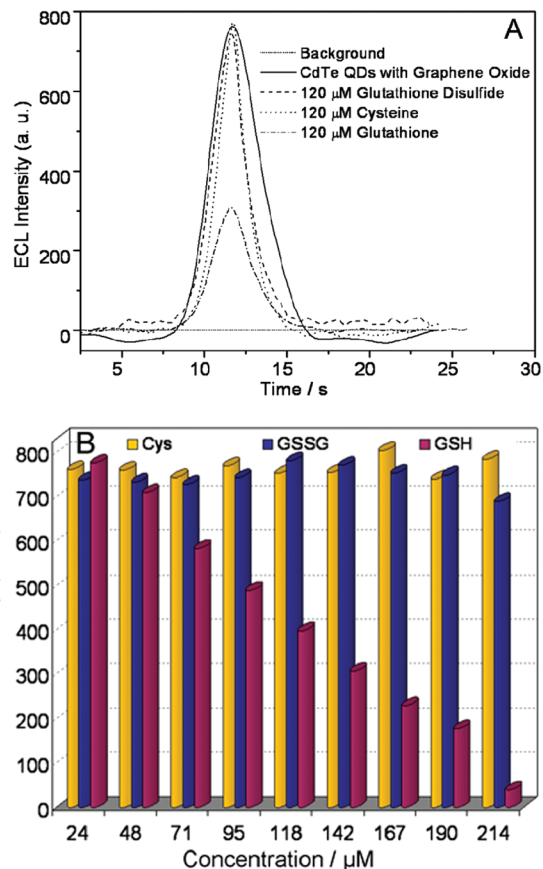


Figure 4. (A) ECL intensity–time behaviors of CdTe QDs with $1.2 \mu\text{g mL}^{-1}$ graphene oxide before (solid line) and after the addition of 120 μM GSSG (dash line), Cys (dot line), and GSH (dash dot line), respectively. (B) ECL responses of CdTe QDs with $1.2 \mu\text{g mL}^{-1}$ graphene oxide to Cys (yellow), GSSG (blue), and GSH (red) with the concentrations of 24, 48, 71, 95, 118, 142, 167, 190, and 214 μM .

Table 1. Calculated Binding Energy between Graphene Oxide and Cysteine (Cys), Glutathione (GSH), and Glutathione Disulfide (GSSG)^a

moiety	GSH (kJ mol^{-1})	GSSG (kJ mol^{-1})	Cys (kJ mol^{-1})
hydroxy	−71.9	13.3	−115.5
epoxy	−117.3	−86.1	−138.0
carboxylic	134.8	−84.7	−103.7

^a Configurations of GSH, Cys, and GSSG were optimized by molecular mechanics after the molecular dynamics simulation with Macromodel software (step size 1.5 fs, simulation time 1 ns). Binding energy was calculated by the PM3 semiempirical method of Gaussian software for GSH, Cys, and GSSG with their optimization configurations.

1 provides the binding energies between the analytes and graphene oxide. The binding energy of GSH was $-54.4 \text{ kJ mol}^{-1}$, much less than that of GSSG ($-147.5 \text{ kJ mol}^{-1}$) and Cys ($-357.2 \text{ kJ mol}^{-1}$). So interferences from Cys and GSSG were eliminated by the big binding energy, and finally the selective detection was realized.

Assays of Real Sample. Glutathione is one of the most important antioxidants, and the glutathione-containing drugs are widely applied in clinics, significant to strengthen immunity, cancer therapies, etc., and take a part in the treatment of human

(50) Stankovich, S.; Dikin, D. A.; Piner, R. D.; Kohlhaas, K. A.; Kleinhammes, A.; Jia, Y.; Wu, Y.; Nguyen, S. T.; Ruoff, R. S. *Carbon* **2007**, *45*, 1558–1565.

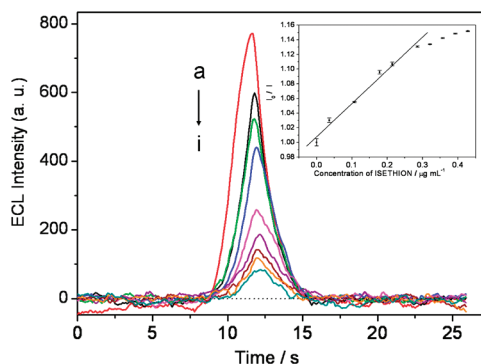


Figure 5. ECL intensity–time behaviors of CdTe QDs with $1.2 \mu\text{g mL}^{-1}$ graphene oxide (a) to the commercial glutathione drug (Isethion) with different concentrations, from curve b to curve i: 0.04, 0.1, 0.18, 0.21, 0.25, 0.29, 0.32, $0.36 \mu\text{g mL}^{-1}$. The inset is the linear relationship between the relative ECL intensity (I_0/I) and the concentration of glutathione. Error bars were calculated from three times parallel experiments. The buffer solution was 0.02 M Na_2CO_3 – NaHCO_3 (pH 9.5); scan rate, 100 mV s^{-1} .

immunodeficiency virus (HIV).⁵¹ Hence, real sample assays about the glutathione-containing drugs are also expected. The proposed ECL platform could realize the direct, sensitive, and continuous detection of the glutathione-containing drug Isethion (Tathion eye drops, Japan). As shown in Figure 5, ECL emission quenched obviously with the drug injection, and the linear relationship (inset of Figure 5) was obtained from 0.04 to $0.43 \mu\text{g mL}^{-1}$. This graphene oxide enhanced CdTe QDs ECL architecture reflected its application in glutathione-containing drug detection, indicating its potentiality in the physiological assays.

(51) Kleinman, W. A.; Richie, J. P. *Biochem. Pharmacol.* **2000**, *60*, 19–29.

CONCLUSION

In conclusion, we have developed an ECL pathway of CdTe QDs with the participation of graphene oxide. Graphene oxide facilitated QDs oxidation and accelerated the output of $\text{O}_2^{\bullet-}$, which could improve the shortcomings of QDs ECL, such as low emission efficiency and unstable radical species. We used the as-prepared ECL platform to realize the sensitive and selective detection of glutathione from thiol-containing compounds and further used it for glutathione drug detection. This work improved the QDs ECL technology, expanded its applications of selective sensing, and predicted the potential abilities of graphene oxide in the analytical methodology.

ACKNOWLEDGMENT

This work was financially supported by the National Natural Science Foundation of China (Nos. 20675044 and 20975060) and the National Basic Research Program of China (Nos. 2007CB310500 and 28-AZC0901).

SUPPORTING INFORMATION AVAILABLE

UV–vis spectra of CdTe QDs and graphene oxide, Mott–Schottky spectra, ECL of CdTe QDs solutions with or without graphene oxide, ECL of CdTe QDs based on a Au electrode, glassy carbon electrode, and ITO electrode, ECL peak height–time responses of methionine, schematic model of a sheet of graphene oxide showing possible oxygen-containing functionalities with the possible hydrogen bonds between glutathione, ball–stick model of glutathione, cysteine, glutathione disulfide, and graphene oxide used for computational chemistry. This material is available free of charge via the Internet at <http://pubs.acs.org>.

Received for review August 26, 2009. Accepted October 30, 2009.

AC901935A